of thermal pressurization of pore fluid and that the gouge behaved like a fluid during high-velocity shearing.

Our experiments show that the Japan Trench décollement material behaves in a manner that promotes further large displacement once high-velocity slip initiates, predominately due to very low shear stress. To understand if this is similar to the behavior of material from other subduction zones, we also performed high-velocity friction experiments on décollement materials for the Nankai Trough (*12*). Like materials from the Japan Trench, the Nankai Trough materials also exhibit lower shear stress in the experiments under impermeable conditions than in those under permeable conditions, consistent with the idea that low-permeability conditions better contain pore fluid so that thermal pressurization occurs more effectively (Fig. 3, A and B). However, when we compare the data obtained under the same experimental conditions for the two different regions, the décollement material from the Japan Trench has overall lower shear stress from peak to steady-state conditions than the material from the Nankai Trough.

The clay content and clay mineralogy of the fault-zone material differs between the Japan Trench and the Nankai Trough (Fig. 3C) (*12*). The décollement of the Nankai Trough developed in the hemipelagic mudstone (*21*), whereas that of the Japan Trench is localized in pelagic clays (*10*). The total clay content in the Nankai décollement is estimated to be 65% (*21*), compared with 85% for the Japan Trench décollement. The smectite content in the Nankai Trough and Japan Trench décollements is 31 and 78% of the total mineralogy, respectively (*12*). Smectite is known as one of the lowest-friction minerals (*22*, *23*). The abundance of smectite means that large slip on the shallow plate-boundary thrust of the Japan Trench can occur more easily than for the Nankai Trough.

Our results indicate that large slip resulted from coseismic weakening of the fault due to the abundance of smectite and thermal pressurization. Seismic slip could be promoted even in unstrained portions at shallow depths, as the slip propagates through the smectite-rich fault material under fluid-saturated, impermeable conditions. Similar pelagic clay is widely distributed on the ocean floor, and plate-boundary décollements have developed in these smectite-rich sediment layers at several subduction zones (*24*, *25*). Such regions also have the potential for very large coseismic displacements on shallow faults, which could generate very large tsunamis similar to the 2011 Tohoku-Oki earthquake.

References and Notes

1. S. L. Bilek, T. Lay, *Geophys. Res. Lett.* **29**, 18-1–18-4 (2002).
2. J. C. Moore, D. Saffer, *Geology* **29**, 183–186 (2001).
3. K. Wang, Y. Hu, *J. Geophys. Res.* **111**, B06410 (2006).
4. S. Ide, A. Baltay, G. C. Beroza, *Science* **332**, 1426–1429 (2011).
5. Y. Ito *et al.*, *Geophys. Res. Lett.* **38**, L00G05 (2011).
6. T. Fujiwara *et al.*, *Science* **334**, 1240 (2011).
7. S. Kodaira *et al.*, *Nat. Geosci.* **5**, 646–650 (2012).
8. Y. Fujii, K. Satake, S. Sakai, M. Shinohara, T. Kanazawa, *Earth Planets Space* **63**, 815–820 (2011).
9. J. Mori, F. M. Chester, N. Eguchi, S. Toczko, *IODP Sci. Prosp.* 343 10.2204/iodp.sp.343.2012 (2012).
10. F. M. Chester *et al.*, *Science* **342**, 1208–1211 (2013).
11. Shipboard Scientific Party, Site 436: Japan Trench outer rise, Leg 56. Vol. 56, 57 (Pt. 1) (1980).
12. Material and methods are available as supplementary materials on *Science* Online.
13. B. J. Skinner, *Geol. Soc. Am.* **97**, 75–96 (1966).
14. R. H. Sibson, *Nature* **243**, 66–68 (1973).
15. C. W. Mase, L. Smith, *J. Geophys. Res.* **92**, 6249–6272 (1987).
16. J. R. Rice, *J. Geophys. Res.* **111**, B05311 (2006).
17. P. M. Fulton *et al.*, *Science* **342**, 1214–1217 (2013).
18. S. Boutareaud *et al.*, *Geophys. Res. Lett.* **35**, L05302 (2008).
19. K. Ujiie, A. Tsutsumi, *Geophys. Res. Lett.* **37**, L24310 (2010).
20. F. Ferri *et al.*, *J. Geophys. Res.* **116**, B09208 (2011).
21. M. Kinoshita *et al.*, in *Proceedings of the Integrated Ocean Drilling Program* (IODP, Tokyo, 2009), vol. 314/315/316; 10.2204/iodp.proc.314315316.133.2009.
22. J. D. Byerlee, *Pure Appl. Geophys.* **116**, 615–626 (1978).
23. M. J. Ikari, D. M. Saffer, C. Marone, *J. Geophys. Res.* **114**, B05409 (2009).
24. A. Maltman, P. Labaume, B. Housen, *Proc. Ocean Drill. Program Sci. Rep.* **156**, 279–292 (1997).
25. H. Tobin, P. Vannucchi, M. Meschede, *Geology* **29**, 907–910 (2001).

Acknowledgments: For this research, we used samples and data provided by the IODP (www.iodp.org/access-data-and-samples). We thank all drilling and logging operation staff on board the *D/V Chikyu* during Expedition 343 and 343T. We acknowledge two anonymous reviewers for their thoughtful reviews. Part of this work was supported by the U.S. Science Support Program of IODP. K.U. was supported by grant 21107005 (Ministry of Education, Culture, Sports, Science and Technology of Japan). E.E.B was supported by the Gordon and Betty Moore Foundation.

Supplementary Materials

www.sciencemag.org/content/342/6163/1211/suppl/DC1
Materials and Methods
Supplementary Text
Figs. S1 to S5
Tables S1 and S2
References (*26*–*30*)

19 July 2013; accepted 30 October 2013
10.1126/science.1243485

Low Coseismic Friction on the Tohoku-Oki Fault Determined from Temperature Measurements

P. M. Fulton,[1]* E. E. Brodsky,[1] Y. Kano,[2] J. Mori,[2] F. Chester,[3] T. Ishikawa,[4] R. N. Harris,[5] W. Lin,[4] N. Eguchi,[6] S. Toczko,[6] Expedition 343, 343T, and KR13-08 Scientists†

The frictional resistance on a fault during slip controls earthquake dynamics. Friction dissipates heat during an earthquake; therefore, the fault temperature after an earthquake provides insight into the level of friction. The Japan Trench Fast Drilling Project (Integrated Ocean Drilling Program Expedition 343 and 343T) installed a borehole temperature observatory 16 months after the March 2011 moment magnitude 9.0 Tohoku-Oki earthquake across the fault where slip was ~50 meters near the trench. After 9 months of operation, the complete sensor string was recovered. A 0.31°C temperature anomaly at the plate boundary fault corresponds to 27 megajoules per square meter of dissipated energy during the earthquake. The resulting apparent friction coefficient of 0.08 is considerably smaller than static values for most rocks.

Earthquake rupture propagation and slip are moderated by the dynamic shear resistance on the fault. Any complete model of earthquake growth therefore requires quantification of shear stress, which is difficult to measure. Historically, the shear stress during an earthquake was thought to nearly equal that controlled by static friction, but recent laboratory experiments and field observations have brought this assumption into question (*1*, *2*). Direct measurement of the magnitude of earthquake stress is challenging because seismological measurements only record stress changes.

Rapid-response drilling provides a solution (*3*). Because the frictional stress during slip results in dissipated heat, subsurface temperature measurements soon after a major earthquake can record the temperature increase over the fault and its decay. If the slip on the fault is known, the thermal observations allow one to infer the frictional shear stress (*4*, *5*). On 15 July 2012, as part of the Japan Trench Fast Drilling Project (JFAST) [Integrated Ocean Drilling Program (IODP) Expedition 343 and 343T], we installed a sub–sea-floor temperature observatory in the

[1]Department of Earth and Planetary Sciences, University of California, Santa Cruz, CA, USA. [2]Disaster Prevention Research Institute, Kyoto University, Kyoto, Japan. [3]Center for Tectonophysics, Department of Geology and Geophysics, Texas A&M University, College Station, TX, USA. [4]Kochi Institute for Core Sample Research, Japan Agency for Marine-Earth Science and Technology, Kochi, Japan. [5]Oregon State University, Corvallis, OR, USA. [6]Center for Deep Earth Exploration, Japan Agency for Marine-Earth Science and Technology, Yokohama, Japan.

*Corresponding author. E-mail: pfulton@ucsc.edu
†Expedition 343, 343T, and KR13-08 Scientists authors and affiliations are listed in the supplementary materials.

Downloaded from http://science.sciencemag.org/ on August 16, 2021

Japan Trench through the plate boundary fault zone (Hole C0019D) (Fig. 1), which was identified through logging and coring in two adjacent boreholes ~30 m away along strike (Holes C0019B and C0019E, respectively) (supplementary text) (*6*). The deep-sea drilling vessel *Chikyu* developed procedures to allow drilling and installation of the observatory at the requisite 6900-m water depth, making it the deepest open-ocean borehole observatory. The observatory consisted of a string of 55 temperature-sensing data loggers with ~0.001°C accuracy that extended beneath the sea floor in a fully cased 4.5-inch-inner-diameter borehole (Fig. 1). Ten of the instruments also recorded pressure at <1 kPa accuracy to provide control on sensor depths.

On 26 April 2013, the Japan Agency for Marine-Earth Science and Technology deep-sea research vessel (R/V) *Kairei* recovered the observatory sensor string with the remotely operated vehicle *Kaiko7000II*. All 55 sensors and the sinker bar were recovered from a maximum depth of 820.6 m below sea floor (mbsf). The water depth of the observatory is ~8 m deeper than the adjacent coring and logging holes, and thus the fault depth relative to the sea floor is expected to be shallower than observed in logging and coring. The successful recovery implies that there was negligible afterslip or distributed deformation in the borehole 16 to 25 months after the mainshock.

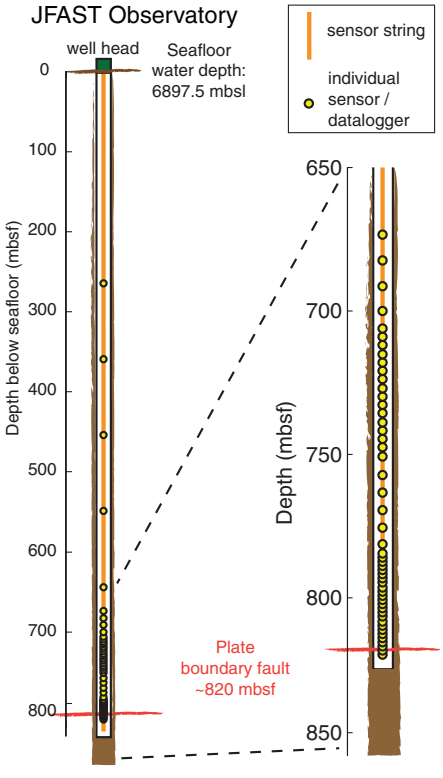

Fig. 1. Observatory configuration. The observatory sensor string of 55 temperature-sensing data loggers attached to a rope was installed within 4.5-inch steel casing that is open at the sea floor and has a check-valve at the bottom preventing inflow of fluid.

The temperature data reveal a background geothermal gradient of 26.29° ± 0.13°C km^{-1} within the region of 650 to 750 mbsf, resulting in a vertical heat flow value of 30.50 ± 2.52 mW m^{-2} when combined with thermal conductivity of 1.16 ± 0.09 W m^{-1} $°C^{-1}$ over this interval (supplementary methods). The temperature from 812 m to the bottom at 820 m is elevated by as much as 0.31°C relative to this background gradient (Fig. 2). This is the largest temperature anomaly within the data set and centered on 819 mbsf at the stratigraphic level estimated for the décollement fault zone (*6*, *7*).

We interpret the temperature anomaly as the frictional heat from the 2011 Tohoku-Oki earthquake. This signal is larger than previous rapid-response measurements of frictional heat across a fault after an earthquake (*4*, *5*) and is temporally resolved so that its transient nature is distinguished. The temperature data record the combination of the background geotherm, the decaying signature of frictional heating during the 2011 Tohoku-Oki earthquake, and transient effects caused by drilling the borehole and hydrologic processes. Low temperatures relative to the background geotherm early in the experiment (Fig. 2) reflect the effects of water circulation during drilling and equilibration of the observatory upon installation. Because this drilling disturbance acts as a line source compared to the plane or slab source from frictional heating on the fault, its characteristic diffusion time is much shorter, allowing measurement of the frictional heat during the 9-month observatory experiment (*8*, *9*) (supplementary text).

To connect the temperature data to the stress on the fault during slip, we modeled the combined effects of the drilling disturbance and frictional heating on the evolution of the temperature field over time and find the energy during the earthquake dissipated as heat that maximizes the normalized cross-correlation between simulations and data (supplementary text and Fig. 3). Parameter values are constrained by independent drilling and material properties data (supplementary text and table S1).

From an inversion exploring a wide range of depths, the preferred location of the frictional boundary is 821.3 mbsf, which is 7718.8 m below mean sea level [7717.8 to 7719.6 mbsl, 90% confidence interval (CI); supplementary text and table S2]. The inversion places the fault below the deepest data logger because the width of the predicted temperature anomaly requires extension to depth for the homogeneous thermal properties used here. However, the peak of the temperature anomaly appears to be above the deepest temperature sensor in the data of Fig. 2, and the width of the anomaly may be governed by a thermal property structure not included in our model. If we constrain the inversion to require the fault to lie near the peak in temperature above the deepest sensor, the preferred location is 819.8 mbsf (7717.3 mbsl). In either case, the inferred depth of the fault in the observatory hole from the frictional heat is above the hard chert as inferred from the rate of penetration during drilling. The fault inferred from the temperature data is at the same stratigraphic level as the plate boundary fault found in the neighboring coring and logging holes (*6*, *7*).

The depth-constrained inversion results in an overlapping range of 27 MJ m^{-2} (19 to 51 MJ m^{-2}, 90% CI) of dissipated frictional heat energy during the earthquake along the plate boundary (Fig. 3). The unconstrained inversion of the temperature observations indicates 31 MJ m^{-2} (20 to 69 MJ m^{-2}, 90% CI) (figs. S4 to S6). In both cases, the dissipated energy in this region of highest slip along the trench (*10*) is comparable to the spatially averaged radiated energy from the earthquake of 6 to 17 MJ m^{-2} (*11*, *12*) (supplementary text).

Alternative interpretations for a positive temperature anomaly around a fault include the effects of locally reduced thermal conductivity or advection of heat by fluid flow up a permeable fault zone. The magnitude and scale of the observed anomaly, however, are unlikely to be the result of thermal-conductivity differences; the high thermal gradient within the ~20 m zone would require a thermal conductivity of 0.73 W m^{-1} $°C^{-1}$, in contrast to values of 1.14 ± 0.07 W m^{-1} $°C^{-1}$ measured on core samples from comparable intervals in hole C0019E. Rather than a large decrease at the fault zone, measurements throughout the hanging wall and footwall intervals covered by the sensors reveal relatively uniform values before a sharp increase to 1.40 ± 0.19 W m^{-1} $°C^{-1}$ within chert beneath the sensor string at >829 mbsf (fig. S2). Assuming similar composition, a value of 0.73 W m^{-1} $°C^{-1}$ would require a bulk porosity of ~80 to 86%. Even if the fault zone is dominated by fractures, such large porosities over tens of meters are unlikely and not supported by logging data or cores recovered from adjacent boreholes.

Fluid flow up a fault conduit may also result in a positive temperature anomaly, as is observed at 784 mbsf (Fig. 2). Generalized models of the effects of fluid flow on a frictional heat signal after an earthquake have shown that large flow velocities resulting from a combination of high permeabilities (>10^{-14} m^2) and driving overpressures are required (*9*). High permeability around 784 mbsf is indicated by resistivity logs and prolonged drilling anomaly decay time (*13*) (fig. S9). Zones of high permeability, most susceptible to the transient drilling disturbance, are also inferred around 765, 800, and 810 mbsf.

None of these indications of high permeability are present at the depth of the inferred slip zone of ~820 mbsf, and additional pore fluid chemistry data confirm that little fluid flow occurs along the plate boundary (supplementary text and fig. S9). The sudden cooling of the anomaly at 784 mbsf after a large local earthquake on 7 December 2012, and the corresponding heating of a high-permeability zone at 763 mbsf, are consistent with the upward propagation of

Downloaded from http://science.sciencemag.org/ on August 16, 2021

a fluid pulse driven by either direct stresses or permeability-altering effects of the December 2012 earthquake that changed the preferred flow path for fluids (*14*, *15*). This interpretation is consistent with borehole images in the interval that show steeply dipping structures conducive to vertical migration of fluids (*13*). Spatially correlated temperature variations within these permeable zones during times of suspected advective fluid flow are suggestive of episodic fluctuations in flow velocity. Such large variations are not observed within the décollement. At 784 mbsf, the standard deviation of roughly daily-to-weekly variability is 100% greater than within the décollement before the December earthquake, and at 763 mbsf it is 60% greater after the earthquake (supplementary text).

The time after the earthquake in which the temperature observations were made is many times as large as the characteristic diffusion time across the slip zone for reasonable estimates of

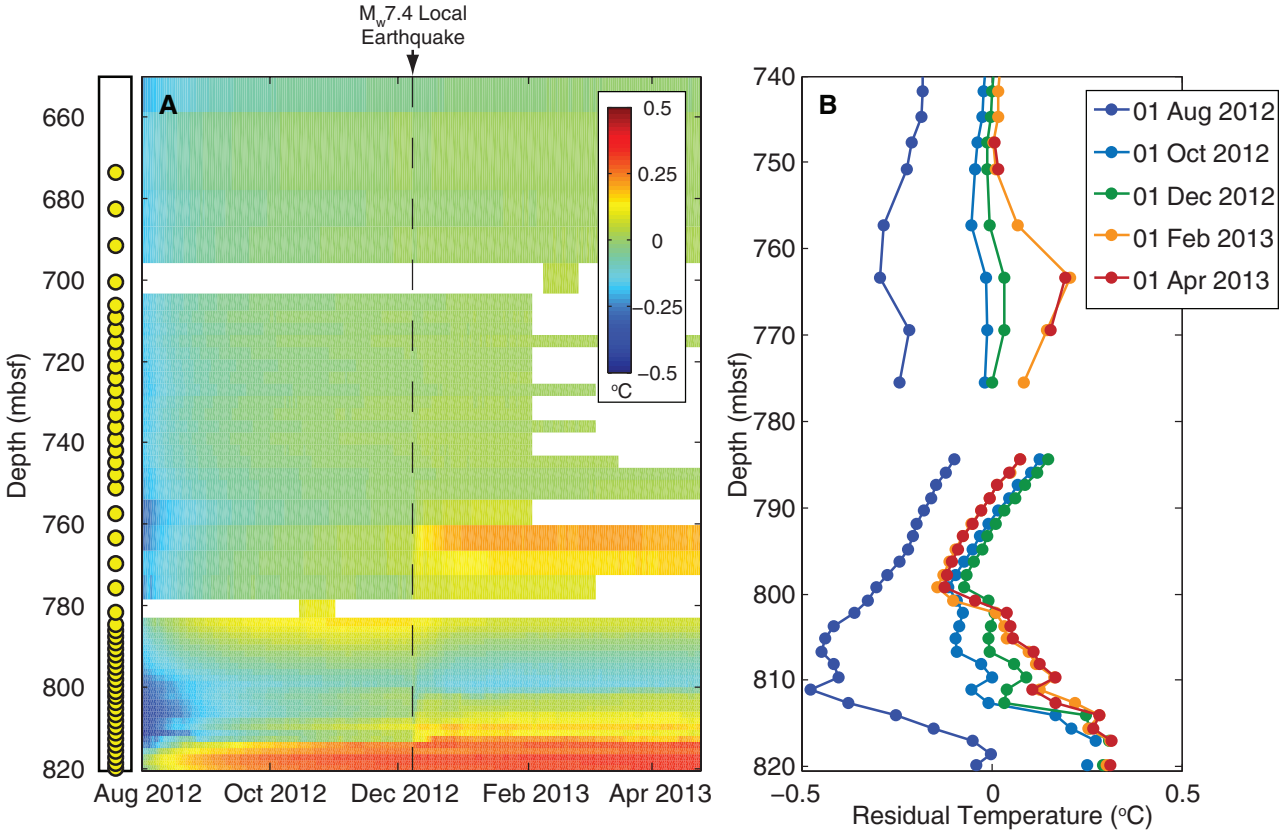

Fig. 2. Sub–sea-floor residual temperature field. (**A**) Time-space map of data >650 mbsf. Yellow dots show sensor positions, and each row represents the corresponding sensor's data. Each column is the daily average temperature after an average background geotherm is removed (supplementary text). A local moment magnitude (M_w) = 7.4 earthquake occurred 17:18:30 Japan Standard Time on 7 December 2012 (dashed line). The second deepest sensor (818.51 mbsf) failed on 22 September 2012; subsequent data in that row are interpolated from sensors 1.5 m above and below. Periods of no data collection are otherwise shown by white. Sensors at 700 and 781 mbsf were programmed to only record for ~2.5-week periods at 1-Hz sampling rate. Data including five broadly spaced shallower depths are included in fig. S1. (**B**) Depth profiles of residual temperature (i.e., with background geotherm removed) from five dates through the experiment separated by 2-month intervals. The times correspond to the vertical tick marks in Fig. 2A. The *y* axis is expanded compared to that in (A) showing data from >740 mbsf. Relatively cool temperatures in August reflect the effects of drilling disturbance.

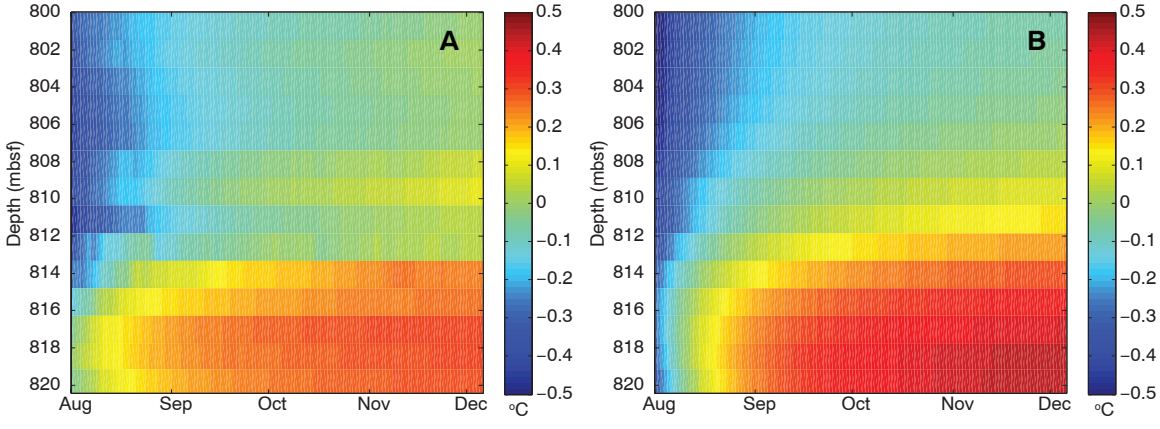

Fig. 3. Time-space map of residual temperature near inferred slip zones. (**A**) A magnified view of Fig. 2A showing the residual temperature anomaly near the plate boundary from 1 August to 6 December 2012. (**B**) Simulated residual temperature from model inversions in which fault depth is constrained. Similar results from an inversion in which fault depth is unconstrained are shown in fig. S4.

Downloaded from http://science.sciencemag.org/ on August 16, 2021

slip zone thickness. Therefore, the measurable temperature anomaly from frictional heating is independent of the slip zone thickness and slip duration and does not directly constrain these parameters (supplementary text). However, by assuming a slip duration ≥50 s and slip zone thickness ≥1 mm, we estimate the maximum peak temperature within the slip zone at this location to be <1250°C (supplementary methods) (fig. S7).

The geotherm itself also provides a constraint on the long-term integrated energy dissipated on the fault zone (*16*, *17*). The conductive vertical heat flux of 30.50 ± 2.52 mW m^{-2} measured here is consistent with subduction thermal models with very little or no long-term displacement-averaged dissipated energy in the form of heat along the plate boundary (*17*).

The dissipated energy is the earthquake parameter best constrained by the temperature data; however, laboratory experiments and theoretical models are often based on the coefficient of friction. For a total of 50 m of slip on the fault (*10*), our best estimate of 27 MJ m^{-2} of local dissipated energy during the earthquake implies an average shear stress of 0.54 MPa. To compare our results to other studies, we assume an effective normal stress of 7 MPa based on the fault's depth, hydrostatic pore pressure, and measured rock densities, to infer the equivalent coseismic coefficient of friction (supplementary text). The resultant apparent coefficient of friction is 0.08. The result is "apparent" because the effective normal stress is inferred from estimates of pore pressure and fault dip (supplementary text). The very low values of shear stress and apparent coefficient of friction, which represent displacement averages during the earthquake, are consistent with values determined from high-velocity (1.3 m s^{-1}) friction experiments on the Japan Trench plate boundary fault material (*18*).

An average shear stress during slip of 0.54 MPa and apparent coefficient of friction of 0.08, as constrained by a measured frictional heat anomaly ~1.5 years after the Tohoku-Oki earthquake, suggest that either friction on the fault is remarkably low throughout the seismic cycle or that there was near total stress release at the JFAST location (*19*, *20*). This very low shear resistance during slip may help explain the large slip at shallow depths that contributed to the large devastating tsunami.

References and Notes

1. J. Byerlee, *Pure Appl. Geophys.* **116**, 615–626 (1978).
2. G. Di Toro *et al.*, *Nature* **471**, 494–498 (2011).
3. E. E. Brodsky, K.-F. Ma, J. Mori, D. M. Saffer, *Sci. Drill.* 10.2204/iodp.sd.8.11.2009 (2009).
4. Y. Kano *et al.*, *Geophys. Res. Lett.* **33**, L14306 (2006).
5. H. Tanaka *et al.*, *Geophys. Res. Lett.* **33**, L16316 (2006).
6. F. M. Chester *et al.*, *Science* **342**, 1208–1211 (2013).
7. The depth interval from which a 1.15-m core of scaly-clay, identified as the fault zone in (*6*), extends from 7709.5 to 7714.3 mbsl in the coring hole 30 m away. In the logging hole, the fault is interpreted at 7709.5 to 7711.5 mbsl, 15 to 17 m above a decrease in rate of penetration associated with entering a hard chert layer at 7726.5 mbsl. A similar decrease in rate of penetration in the observatory hole is observed at 7727.5 mbsl. All depth correlations between holes contain an estimated several meters of uncertainty due to fluctuations of the ship's absolute elevation, flexure of the 7 km of drill stand, borehole deviation, layer-thickness variations, and fault dip.
8. E. Bullard, *Geophys. J. Int.* **5**, 127–130 (1947).
9. P. M. Fulton, R. N. Harris, D. M. Saffer, E. E. Brodsky, *J. Geophys. Res.* **115**, B09402 (2010).
10. T. Fujiwara *et al.*, *Science* **334**, 1240–1240 (2011).
11. T. Lay, H. Kanamori, *Phys. Today* **64**, 33–39 (2011).
12. S. Ide, A. Baltay, G. C. Beroza, *Science* **332**, 1426–1429 (2011).
13. F. M. Chester, J. J. Mori, S. Toczko, N. Eguchi, the Expedition 343/343T Scientists, Japan Trench Fast Drilling Project (JFAST). *IODP Proceedings* 343/343T (2013).
14. C.-Y. Wang, M. Manga, *Earthquakes and Water*, vol. 114, Lecture Notes in Earth Sciences (Springer, Berlin, 2010).
15. J. E. Elkhoury, E. E. Brodsky, D. C. Agnew, *Nature* **441**, 1135–1138 (2006).
16. K. Wang, T. Mulder, G. C. Rogers, R. D. Hyndman, *J. Geophys. Res.* **100**, 12907–12918 (1995).
17. G. Kimura *et al.*, *Earth Planet. Sci. Lett.* **339-340**, 32–45 (2012).
18. K. Ujiie *et al.*, *Science* **342**, 1211–1214 (2013).
19. K. Wang, K. Suyehiro, *Geophys. Res. Lett.* **26**, 2307–2310 (1999).
20. W. Lin *et al.*, *Science* **339**, 687–690 (2013).

Acknowledgments: We thank all drilling and operations staff on board the deep-sea drilling vessel *Chikyu* during IODP Expedition 343 and 343T and R/V *Kairei* during KR12-16, KR13-04, and KR13-08, operated by Japan Agency for Marine-Earth Science and Technology. The data are provided by IODP via CDEX (www.iodp.org/access-data-and-samples). The data analysis is funded by the Gordon and Betty Moore Foundation through grant GBMF3289 to E.E.B.

Supplementary Materials

www.sciencemag.org/content/342/6163/1214/suppl/DC1
Materials and Methods
Supplementary Text
Figs. S1 to S9
Tables S1 and S2
References (*21*–*26*)

23 July 2013; accepted 30 October 2013
10.1126/science.1243641

Giant Convection Cells Found on the Sun

David H. Hathaway,[1]* Lisa Upton,[2,3] Owen Colegrove[4]

Heat is transported through the outermost 30% of the Sun's interior by overturning convective motions. These motions are evident at the Sun's surface in the form of two characteristic cellular structures: granules and supergranules (~1000 and ~30,000 kilometers across, respectively). The existence of much larger cells has been suggested by both theory and observation for more than 45 years. We found evidence for giant cellular flows that persist for months by tracking the motions of supergranules. As expected from the effects of the Sun's rotation, the flows in these cells are clockwise around high pressure in the north and counterclockwise in the south and transport angular momentum toward the equator, maintaining the Sun's rapid equatorial rotation.

The Sun, like most stars, has an outer convection zone in which heat generated by nuclear reactions in its core is transported to its surface by overturning convective motions. These motions were evident in early telescopic observations of the Sun as granules, which are bright grain-like structures with typical diameters of ~1000 km, lifetimes of ~10 min, and flow velocities of ~3000 m s^{-1}. Much larger structures—supergranules—were evident from their flow velocities, as seen in the Doppler shift of atomic spectral lines formed in the Sun's surface layers (*1*, *2*). Supergranules have diameters of ~30,000 km, lifetimes of ~24 hours, and flow velocities of ~500 m s^{-1}. Both granules and supergranules cover the entire solar surface but are substantially modified by the intense magnetic fields in and around sunspots.

The existence of even larger convection cells—giant cells—was proposed shortly after supergranules were detected (*3*). These cells are expected to span the 200,000-km-deep solar convection zone, to have diameters of ~200,000 km and lifetimes of ~1 month, and to be heavily influenced by the Sun's 27-day rotation. Hydrodynamical models of convective motions in the Sun's rotating convection zone (*4*–*6*) suggest that these cells should be elongated north-to-south near the equator and be sheared off at higher latitudes by the Sun's differential rotation (the equatorial regions rotate once in ~25 days, whereas the polar regions rotate once in ~35 days). These "banana" cells should transport angular momentum toward the Sun's equator—a critically important process for maintaining the differential rotation.

The observational evidence for the existence of giant cells has been only suggestive. Magnetic structures of a similar size and shape have been

[1]NASA Marshall Space Flight Center, Huntsville, AL 35812, USA. [2]Department of Physics and Astronomy, Vanderbilt University, Nashville, TN 37235, USA. [3]Department of Space Science, University of Alabama in Huntsville, Huntsville, AL 35899, USA. [4]Department of Physics and Astronomy, University of Rochester, Rochester, NY 14627, USA.

*Corresponding author. E-mail: david.hathaway@nasa.gov

Downloaded from http://science.sciencemag.org/ on August 16, 2021

Science

Low Coseismic Friction on the Tohoku-Oki Fault Determined from Temperature Measurements

P. M. Fulton, E. E. Brodsky, Y. Kano, J. Mori, F. Chester, T. Ishikawa, R. N. Harris, W. Lin, N. Eguchi, S. Toczko and Expedition 343, 343T, and KR13-08 Scientists

Science **342** (6163), 1214-1217.
DOI: 10.1126/science.1243641

Deep Drilling for Earthquake Clues

The 2011 M_W 9.0 Tohoku-Oki earthquake and tsunami were remarkable in many regards, including the rupturing of shallow trench sediments with huge associated slip (see the Perspective by **Wang and Kinoshita**). The Japan Trench Fast Drilling Project rapid response drilling expedition sought to sample and monitor the fault zone directly through a series of boreholes. **Chester *et al.*** (p. 1208) describe the structure and composition of the thin fault zone, which is predominately comprised of weak clay-rich sediments. Using these same fault-zone materials, **Ujiie *et al.*** (p. 1211) performed high-velocity frictional experiments to determine the physical controls on the large slip that occurred during the earthquake. Finally, **Fulton *et al.*** (p. 1214) measured in situ temperature anomalies across the fault zone for 9 months, establishing a baseline for frictional resistance and stress during and following the earthquake.

ARTICLE TOOLS http://science.sciencemag.org/content/342/6163/1214

SUPPLEMENTARY MATERIALS http://science.sciencemag.org/content/suppl/2013/12/04/342.6163.1214.DC2
http://science.sciencemag.org/content/suppl/2013/12/04/342.6163.1214.DC1

RELATED CONTENT http://science.sciencemag.org/content/sci/342/6163/1178.full
http://science.sciencemag.org/content/sci/342/6163/1208.full
http://science.sciencemag.org/content/sci/342/6163/1211.full
http://science.sciencemag.org/content/sci/342/6163/1262.2.full

REFERENCES This article cites 20 articles, 6 of which you can access for free
http://science.sciencemag.org/content/342/6163/1214#BIBL

PERMISSIONS http://www.sciencemag.org/help/reprints-and-permissions

Use of this article is subject to the Terms of Service

Science (print ISSN 0036-8075; online ISSN 1095-9203) is published by the American Association for the Advancement of Science, 1200 New York Avenue NW, Washington, DC 20005. The title *Science* is a registered trademark of AAAS.

Copyright © 2013, American Association for the Advancement of Science

Downloaded from http://science.sciencemag.org/ on August 16, 2021